Molecular Crystals and Liquid Crystals

ISSN: 1542-1406 (Print) 1563-5287 (Online) Journal homepage: http://www.tandfonline.com/loi/gmcl20

Calculation of Ray Path in Liquid Crystal Modes

Byung-June Mun, Sung-Ho Youn, Joun Ho Lee, Byeong Koo Kim, Hyun Chul Choi, Bongsoon Kang & Gi-dong Lee

To cite this article: Byung-June Mun, Sung-Ho Youn, Joun Ho Lee, Byeong Koo Kim, Hyun Chul Choi, Bongsoon Kang & Gi-dong Lee (2015) Calculation of Ray Path in Liquid Crystal Modes, Molecular Crystals and Liquid Crystals, 613:1, 75-81, DOI: 10.1080/15421406.2015.1032056

To link to this article: http://dx.doi.org/10.1080/15421406.2015.1032056

Published online: 06 Jul 2015.

Mol. Cryst. Liq. Cryst., Vol. 613: pp. 75–81, 2015

ISSN: 1542-1406 print/1563-5287 online
DOI: 10.1080/15421406.2015.1032056

Taylor & Francis
Taylor & Francis Group

Calculation of Ray Path in Liquid Crystal Modes

BYUNG-JUNE MUN,[1] SUNG-HO YOUN,[1,2] JOUN HO LEE,[2] BYEONG KOO KIM,[2] HYUN CHUL CHOI,[2] BONGSOON KANG,[1] AND GI-DONG LEE[1,*]

[1]Department of Electronics Engineering, Dong-A University, Busan, South Korea
[2]LG Display Co., Ltd., Gumi, Gyung-buk, South Korea

In this paper, we introduce the optical approach for the calculation of optical path in arbitrary aligned birefringence media for controlling the incident light, and also calculate the ray path in representative liquid crystal (LC) modes. In calculation, we multi-dimensionally calculated the Poynting vector ***S*** *and wave vector* ***k*** *of ordinary and extra-ordinary rays, and considered both y-axis and z-axis interfaces by using the dielectric tensor rotation method. Finally, we could achieve the exact ray path in various LC modes, and confirmed the propagating direction of the light according to azimuth angles in LC layers.*

Keywords Liquid crystal; Ray path; Poynting vector; Phase matching method; electrically controlled birefringence; azimuth angle

1. Introduction

Various liquid crystal (LC) modes, such as twisted nematic (TN), vertical alignment (VA), in-plane switching (IPS), fringe-field switching (FFS), have been studied to improve the image quality of LCDs [1–7]. Optical technologies regarding LC modes were focused on calculating the phase and transmittance of the light so far. However, current study for the LC technology is requiring the calculation of the ray path because various LC modes are becoming to use as ray path controlling device such as tunable lens. Therefore, exact calculation of ray path of the ordinary (o) and extraordinary (e) waves of the light passing through LC modes become more important. In order to calculate the ray path of the light in LC modes, the characteristics of the arbitrary aligned LC modes must check firstly. In general, LC modes consist of many birefringence layers whose orientations of LC directors are continuously changed between neighbouring LC directors in polar and azimuth direction between two isotropic substrates. Therefore, exact ray position of the light after passing through the LC mode should be obtained after important calculation; refraction and reflection at the interface between isotropic and uniaxial birefringence layer, between inhomogeneous uniaxial to uniaxial layer. Moreover, the ray path in LC modes may be more complicate because the o-ray and e-ray are liable to become bundle rays during pass through multi-dimensional aligned LC modes. Therefore, the calculation of the refraction property as a function of the difference of the director orientation between

*Address correspondence to Gi-Dong Lee, Department of Electronics Engineering, Dong-A University, Busan 604-714, South Korea. E-mail: gdlee@dau.ac.kr

the neighbouring LC molecules is important for simple and exact calculation. In previous paper, we handled the calculation of ray path for e-ray and o-ray in an arbitrary orientational interface at each axis by using the phase matching method [8]. From the simple calculation in TN cell, this optical approach could guarantee the calculation of the exact ray path in arbitrary LC orientation state.

In this paper, we calculated the ray path of the light in representative LC modes to obtain the good properties of tunable LC lens by using the phase-matching method. By calculating the direction of the e-ray and o-ray when the orientation of LC directors in each mode is continuously changed as a function of the applied voltage state, we control the ray path of the light in the LC modes, and the optical performance of LC modes could be analysed from the calculation in this paper.

2. Theory for Calculation of Ray Path of the Light in Arbitrary Aligned LC Mode in Multi-Dimensional Interfaces

In general, LC modes exist as two multi-dimensional interfaces, which are an isotropic-uniaxial (I-U) medium and a uniaxial-uniaxial (U-U) medium. The electric field **E** in anisotropic media such as LC modes is not equal to the dielectric displacement vector **D** caused by dielectric tensor ε, which is represented at *xyz*-coordinate system as $\varepsilon = R(\theta, \varphi)\varepsilon R(\theta, \varphi)^{-1}$, and $R(\theta, \varphi)$ is rotational matrix and the polar angle θ and azimuth angle φ define the optical axis of the LC directors in modes. Assuming that the LC layer are inhomogenously aligned along the *y*-*z* plane on each layer, we can decide the coordinate rotation matrix at *y*-*z* plane to solve the tensor ε.

Basically, incident light in birefringence media of LC mode can be divided into e-wave and o-wave. All rays of o-wave in LC layer can be calculated from the Snell's law because of isotropic properties. However, e-wave does not obey the Snell's law so we should solve the wave equation to achieve the ray path vector, which means the Poynting vector **S**. Figure 1(a) and 1(b) show the relation of the e-wave vector $\boldsymbol{k_e}$ and the Poynting vector **S** at anisotropic interface and boundary condition for achieving the angle θ_e. We could calculate

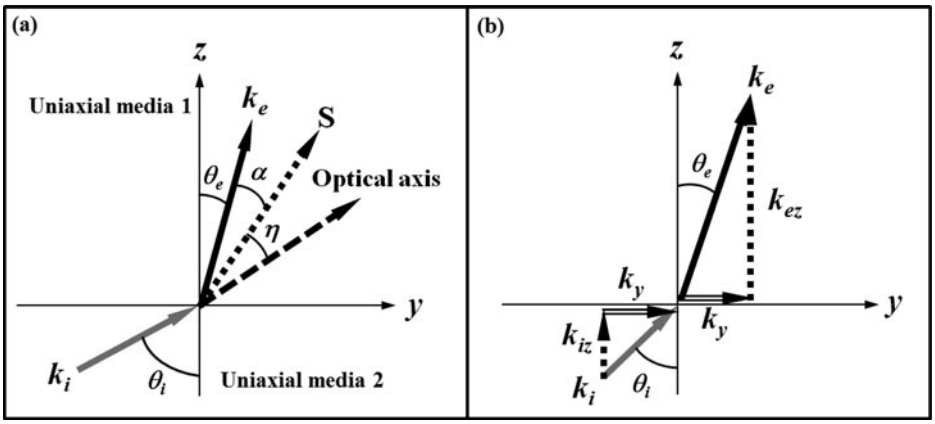

Figure 1. (a) The relation of the e-wave vector $\boldsymbol{k_e}$ and the Poynting vector **S** at uniaxial to uniaxial medium interface and (b) the boundary condition for achieving the angle θ_e.

the Poynting vector S as shown in the following equation [8, 9]:

$$S = ((\sin\theta_e \hat{y} + \cos\theta_e \hat{z}) \sin(\eta + \alpha)) / \sin(\eta) - (\sin\theta cos\phi + \cos\phi \hat{z}) \quad (1)$$

where, θ_e is angle between the vector $\boldsymbol{k_e}$ and the z-axis, and the dispersion angle α is a difference angle between the vector $\boldsymbol{k_e}$ and vector **S**. The η which is the angle between the optical axis of LC layer and the $\boldsymbol{k_e}$ could be calculated by using the equation $\cos^{-1}(\sin\theta \cos\varphi \sin\theta_e + \cos\theta \cos\theta_e)$. As shown in Fig. 1, the vector **S** can be determined by angle η, α, and θ_e.

We first consider the angle θ_e for the I-U and U-U medium, respectively. In the I-U interface, the angle θ_e is easily calculated by relation between $\boldsymbol{k_y}$ and $\boldsymbol{k_{ez}}$ with $\theta_e = \tan^{-1}(\boldsymbol{k_y}/\boldsymbol{k_{ez}})$. The vector $\boldsymbol{k_y}$ is simply calculated from the equation $n(\sin\theta_i)$ by boundary condition in Fig. 1(b), and $\boldsymbol{k_{ez}}$ is calculated by using the wave equation which is expressed into two quadratic equations [8–10]. On the other hand, the refractive index (n) at U-U interface is changed depending on the incident direction so that the vector $\boldsymbol{k}_y$ could be represented as $n_{eff}(\theta, \varphi)\sin\theta_i$. The n_{eff} which is effective refractive index can be calculated using the follow equation [11],

$$n_{eff}(\theta, \phi) = (n_e n_o) / \sqrt{\left(n_o^2 - \left(n_o^2 + n_e^2\right)(\sin\theta cos\phi \sin\theta_e + \cos\theta \sin\theta_e)^2\right.} \quad (2)$$

Then, the dispersion angle α in incident plane which is correlated by vector $\boldsymbol{k_e}$ and optical axis in LC layer can be achieved using the equation $\tan^{-1}((\varepsilon_e - \varepsilon_o) \tan\eta / (\varepsilon_e + \varepsilon_o \tan^2\eta))$. Finally, we can calculate the Poynting vector **S** of e-wave in anisotropic media from the calculated angle α and η.

Figure 2 shows the incident and output wave vector **k** at two interfaces. The calculated Poynting vector **S** of an e-wave should consider y and z-axis interface depending on the

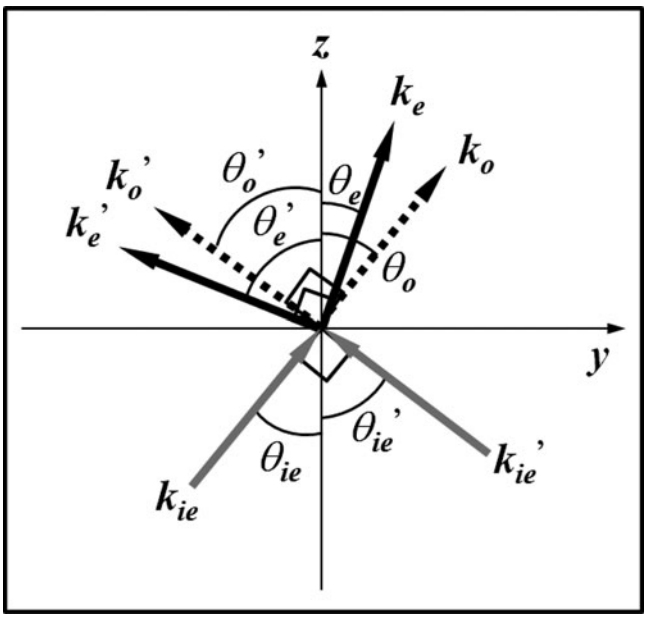

Figure 2. Illustration of rotated direction of wave vector **k**, at two interfaces.

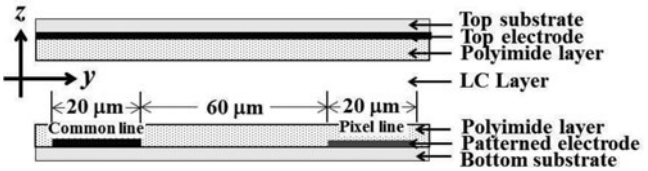

Figure 3. Schematic diagram of the cell and electrode structure for calculation of ray path in LC modes.

light passing through the LC layer. To solve this simple problems, we used the dielectric tensor rotation method as following equation: $\varepsilon = R(\theta_r)R(\theta, \varphi)\varepsilon R(\theta, \varphi)^{-1}R(\theta_r)^{-1}$. Here, $R(\theta_r)^{-1}$ represents the electric tensor rotation matrix and angle θ_r is defined as 90° due to the orthogonality between y-axis and z-axis. Consequently, we can simply calculate the angles $\theta_e{}'$ and $\theta_o{}'$ at y-axis interface by rotating the 90° after determining the θ_e and θ_o at z-axis interface. This dielectric tensor rotation method can provide the multi-dimensional ray tracing in birefringence medium so that the calculation of ray path of the light in all LC modes can be performed by applying this method.

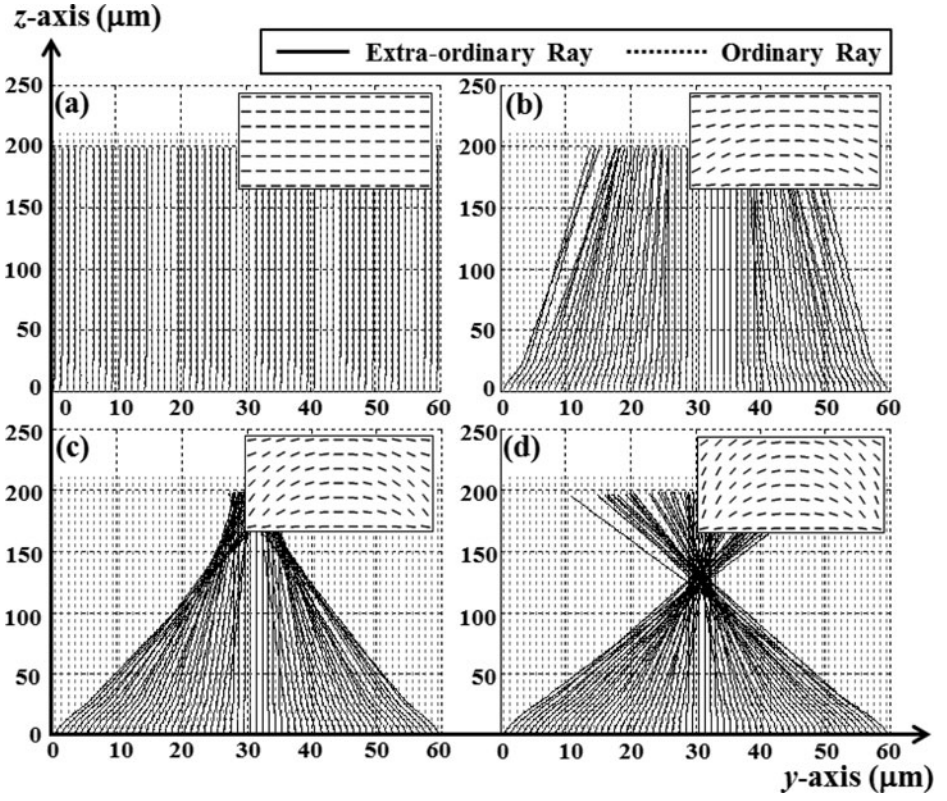

Figure 4. The calculated ray path of wave vector $\boldsymbol{k_e}$ and $\boldsymbol{k_o}$ in an electrically controlled birefringence (ECB) mode as a fucntion of the applied voltage: (a) 0 V, (b) 4 V, (c) 5 V and (d) 6 V.

3. Calculation for Ray Path of the Light in LC Modes

To demonstrate the proposed optical approach for calculation of ray path in birefringence media, we first calculate the propagation of rays in LC lens cell depending on the applied voltages. Figure 3 shows the cross-sectional view of the structure for tunable LC lens cell. The electrode width of both the common and the pixel line is 20 μm and distance between two electrodes is set to 60 μm, respectivley. Top electrode has common electrode. The cell gap is set to 30 μm.

Figure 4 shows the calculated rays of wave vector $\boldsymbol{k_e}$ and $\boldsymbol{k_o}$ in the LC lens cell at y-z interface [12, 13]. The inset in Fig. 4 presents the calculated profile of LC director (Merck, MAT-10-566, $\Delta n = 0.2276$, $n_{\mathrm{o}} = 1.5219$, $n_{\mathrm{e}} = 1.7495$, $\Delta\varepsilon = 6.6$) in the LC lens cell at each applied voltage. We desinged the tunable LC lens using an electrically controlled birefringence (ECB) mode (the azimuth angle $\varphi = 0^{\circ}$) which has a focal length of 125 μm [14, 15]. In the inital state in Fig. 4(a), the solid lines, which represent the extra-ordinary ray, are propagating along the z-axis in LC layer without any change of path due to the homogeneous state. After applied the voltage in LC lens cell in Fig. 4(b) and 4(c), rays are slightly gathering because of the symemetrical alignment of the LC directors along the z-axis. Finally, we observed that all rays in the LC lens cell at 6 V are focused at 125 μm as shown in Fig. 4(d). On the contrary, the ordinary ray which is dotted line straightly propagated without change of voltages because of the isotropic properties of LC lens cell.

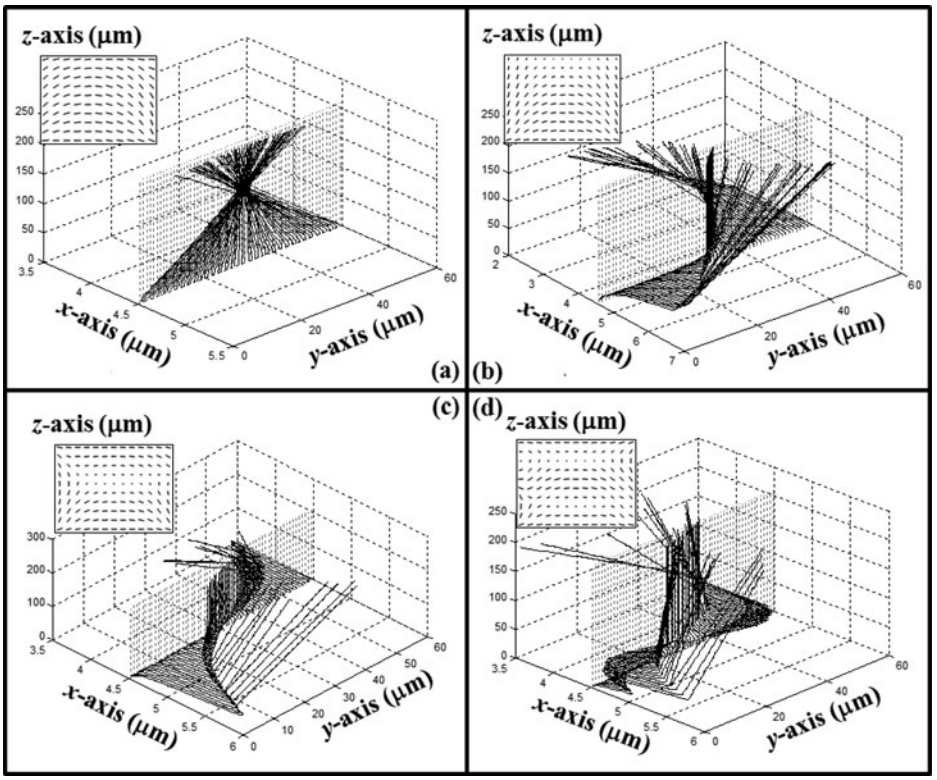

Figure 5. The calculated ray path of the extraordinary and the ordinary waves in LC lens cell if the azimuth angle φ is (a) 0°, (b) 90°, (c) 180° and (d) 360°.

Additionally, we confirmed that all rays always stay on the y-axis because the azimuth angle is 0°. As a result, we can expect that the azimuth angle φ in LC cell is closely related to propagating direction of rays in birefringence media.

To demonstrate the relation between the azimuth angle φ of LC directors and the propagating direction of rays in multi-dimensional birefringence media, we calculated the ray path in the LC lens cell with azimuth angle φ. In case of LC lens cell with zero azimuth angle in Fig. 5(a), extra-ordinary rays are propagated along the z-direction without any twist of ray directions. However, propagating extra-ordinary rays at the azimuth angle 90° in Fig. 5(b) move to both x-axis and y-axis and also not focused. Especially, we can observe that extra-ordinary rays are more twisted when the azimuth angle is increased as shown in Fig. 5(c) and 5(d) so that rays were also not focused in arbitrary aligned LC layers. Consequently, arbitrary aligned LC layers with azimuth angle φ were not used as LC lens cell becasue of the change of ray directions by the azimuth angles.

4. Conclusion

In summary, we reported the optical approach for calculation of ray path in an inhomogeneously aligned LC mode. To achieve the extra-ordinary rays in the inhomogeneous LC layer, we solve the wave vector **k** and Poynting vector **S** in I-U and U-U interfaces by using the phase matching method. We also considered both y-axis and z-axis interfaces from the dielectric tensor rotation method so that the exact calculation of ray path could be possible. From the optical approach, we calculated the propagation of rays in LC lens cell depending on the applied voltages and also demonstrated the ray focusing properties in LC lens cell with/without azimuth angle φ. As results, we could confirm that the change of azimuth angle in LC layer induces change of propagating direction of rays so that we finally proven that arbitrary aligned LC layers with azimuth angle φ were not used as LC lens cell becasue of the change of ray directions by the azimuth angles.

Funding

This research was supported by Dong-A University research fund.

References

[1] Schadt, M., & Helfrich, W. (1971). *Appl. Phys. Lett.*, *18*, 127.
[2] Wu, S.-T., Efron, U., & Hess, L. D. (1984). *Appl. Phys. Lett.*, *44*, 842.
[3] Kim, S. G.., Kim, S. M., Kim, Y. S., Lee, H. K., Lee, S. H., Lee, G.-D., Lyu, J.-J. & Kim, K. H. (2007). *Appl. Phys. Lett.*, *90*, 261910.
[4] Mun, B.-J., Jin, T. Y., Lee, G.-D., Lim, Y. J. & Lee, S. H. (2013). *Opt. Lett.*, *38*, 799.
[5] Oh-e, M., & Kondo, K. (1995). *Appl. Phys. Lett.*, *67*, 3895.
[6] Lee, S. H., Lee, S. L., & Kim, H. Y. (1998). *Appl. Phys. Lett.*, *73*, 2881.
[7] Lim, Y. J., Lee, M.-H., Lee, G.-D., Jang, W.-G., & Lee, S. H. (2007) *J. Phys. D: Appl. Phys.*, *40*, 2759–2764.
[8] Youn, S.-H., Mun, B.-J., Lee, J. H., Kim, B. K., Choi, H. C., Lee, S. H., Kang, B., & Lee, G.-D. (2014). *J. Mod. Opt.*, *61*, 257.
[9] Cojocaru, E. (1997). *Appl. Opt.*, *36*, 302.
[10] Yeh, P., & Gu, C. *Optics of Liquid Crystal Displays* (Wiley Interscience, 1999), Chap. 3, p. 46.
[11] Liang, Q.-T. (1990). *Appl. Opt.*, *29*, 1008–1010 .
[12] Sonehara, T., (1990). *Jpn. J. Appl. Phys.*, *29*(7), L1231.

[13] Itoh, Y., Seki, H., Uchida, T., & Masuda, Y. (1991). *Jpn. J. Appl. Phys.*, *30*(7B), L1296 .
[14] Mun, B.-J., Back, J.-H., Lee, J. H., Kim, B. K., Choi, H. C., Kim, J.-H., & Lee, G.-D. (2013). *IEEE Trans. Electron Devices*, *60*, 3430–3434.
[15] Goodman, J. W., *Introduction to Fourier Optics*. New York, NY, USA: McGraw-Hill, (1968).